

Phase structure of Z_2 gauge theories for frustrated antiferromagnets in two dimensions

Kazuya Nakane, Akihiro Shimizu, and Ikuo Ichinose

Department of Applied Physics, Graduate School of Engineering, Nagoya Institute of Technology, Nagoya 466-8555, Japan

(Received 24 September 2009; revised manuscript received 30 November 2009; published 30 December 2009)

In this paper, we study phase structure of Z_2 lattice gauge theories that appear as an effective-field theory describing low-energy properties of frustrated antiferromagnets in two dimensions. Spin operators are expressed in terms of Schwinger bosons, and an emergent U(1) gauge symmetry reduces to a Z_2 gauge symmetry as a result of condensation of a bilinear operator of the Schwinger boson describing a short-range spiral order. We investigated the phase structure of the gauge theories by means of the Monte Carlo simulations, and found that there exist three phases, phase with a long-range spiral order, a dimer state, and a spin liquid with deconfined spinons. Detailed phase structure and properties of phase transitions depend on details of the models.

DOI: 10.1103/PhysRevB.80.224425

PACS number(s): 75.50.Ee, 11.15.-q, 75.10.Jm

I. INTRODUCTION

In the last few decades, strongly correlated electron systems are one of the most intensively studied areas in the condensed-matter physics. One may expect that some exotic phase appears as a result of the interplay of strong correlations and quantum fluctuations. Concerning to the high- T_c cuprates, understanding of the underdoped regime is still controversial. Conventional Fermi-liquid picture may not hold in that region.¹

Another intensively studied system is quantum magnets with frustrations. Study of that system has long history but its interests recently revived because very interesting experiments on the new materials such as the organic Mott insulators κ -(ET)₂Z (Z =Cu[N(CN)₂]Cl, etc.) (Ref. 2) and X [Pd(dmit)₂]₂ (X =Me₄P, etc.) (Refs. 3–5) have appeared. Among them, the insulator with Z =Cu₂(CN)₃ has no long-range order (LRO) at low temperature^{6,7} and it is expected that a new type of spin liquid, so-called Z_2 spin liquid, is realized there.⁸ Another interesting anisotropic triangular antiferromagnet is Cs₂CuCl₄. By neutron scattering, its spinon-like behaviors were observed.^{9,10}

To study possibility of exotic states in frustrated antiferromagnets such as the Z_2 spin liquid, most studies employ the Schwinger-boson representation for quantum spin operator. As a result, there appear a local U(1) gauge symmetry and also an emergent gauge field. Dynamics of the emergent gauge field strongly influences the structure of the ground-state and low-energy excitations. In the Z_2 spin-liquid scenario, the U(1) gauge symmetry is reduced to a Z_2 symmetry because of appearance of a short-range spin spiral order, and $s=\frac{1}{2}$ spinons are deconfined and appear as a low-energy excitation.¹¹ In order to obtain a conclusive proof of the existence of the Z_2 spin liquid, reliable investigation on the gauge dynamics is necessary. In the present paper, we shall report results of study on the Z_2 gauge theories obtained mostly by means of the Monte Carlo (MC) simulations.

The present paper is organized as follows. In Sec. II, we shall introduce models of frustrated antiferromagnets and review the Schwinger-boson representation of them. We show that their low-energy effective model is a CP¹ gauge model coupled with an additional doubly charged vector field de-

scribing a short-range spiral order. In Sec. III, we shall show the phase structure of various effective gauge models with local Z_2 gauge symmetry. To obtain the phase diagrams, we calculated “internal energy,” “specific heat,” spin-correlation functions, and instanton density by means of MC simulations. There are three phases, phase with long-range order, dimer phase, and spin liquid with deconfined spinons. Section IV is devoted for conclusion and discussion.

II. FRUSTRATED ANTIFERROMAGNETS, SCHWINGER BOSON, AND EFFECTIVE GAUGE THEORY

A. AF magnets and CP¹ gauge-field theory

Let us start with some specific model of a frustrated antiferromagnet on the triangular lattice shown in Fig. 1. Exchange coupling in the horizontal bond is J' and the others are J . Quantum Hamiltonian \mathcal{H} is given as

$$\mathcal{H} = J \sum \vec{S}_i \cdot \vec{S}_j + J' \sum \vec{S}_i \cdot \vec{S}_j + \dots, \quad (2.1)$$

where \vec{S}_i is $s=\frac{1}{2}$ spin operator at site i , and the ellipsis denotes multispin and/or long-range interactions between spins, and the other notations are self-evident.

In the limit $J'/J \ll 1$, the system reduces to the usual antiferromagnets on the square lattice and the ground state is expected to have the Néel order whereas for $J'/J \sim 1$, a new state is expected to appear. In order to study the system [Eq. (2.1)] by field-theory methods, we introduce the Schwinger-boson operators $a_i=(a_{\uparrow i}, a_{\downarrow i})$ at each site i , and then \vec{S}_i is expressed as

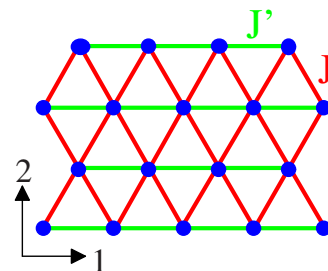


FIG. 1. (Color online) Triangular lattice on which the Heisenberg model (2.1) is defined.

$$\vec{S}_i = \frac{1}{2} a_i^\dagger \vec{\sigma} a_i, \quad (2.2)$$

where $\vec{\sigma}$ are the Pauli spin matrices. The following local constraint must be imposed as the physical-state condition in the Schwinger-boson Hilbert space,

$$(a_{\uparrow i}^\dagger a_{\uparrow i} + a_{\downarrow i}^\dagger a_{\downarrow i}) |\text{Phys}\rangle = |\text{Phys}\rangle. \quad (2.3)$$

We employ the path-integral methods to investigate the quantum system, and introduce CP¹ variables $z_i = (z_{\uparrow i}, z_{\downarrow i}) = (z_{1i}, z_{2i})$ corresponding to a_i , which satisfy the constraint

$$\bar{z}_{\uparrow i} z_{\uparrow i} + \bar{z}_{\downarrow i} z_{\downarrow i} = 1 \quad (2.4)$$

at each site i and $\bar{z}_{\uparrow, \downarrow, i}$ is the complex conjugate of $z_{\uparrow, \downarrow, i}$. From Hamiltonian (2.1), the partition function is given as

$$Z = \int [D\bar{z}Dz]_{\text{CP}^1} \exp \left[- \int d\tau \left(\sum_i \bar{z}_i \cdot \dot{z}_i + \mathcal{H}(\bar{z}, z) \right) \right], \quad (2.5)$$

where τ is the imaginary time, $\dot{z}_i = \frac{dz_i}{d\tau}$ and $\int [D\bar{z}Dz]_{\text{CP}^1}$ denotes the integration over CP¹ variables z_i 's satisfying the constraint [Eq. (2.4)]. $\mathcal{H}(\bar{z}, z)$ is derived from Eqs. (2.1) and (2.2). The above system is obviously invariant under a *local gauge transformation* $z_i(\tau) \rightarrow e^{i\theta_i(\tau)} z_i(\tau)$ with an arbitrary $\theta_i(\tau)$ satisfying $\theta_i(+\infty) = \theta_i(-\infty)$.

In the limit $J' \rightarrow 0$, an effective-field theory is obtained from the partition function Z in Eq. (2.5) by integrating out the high-energy modes of z_i (or z_i 's on all odd sites^{12,13}). The resultant theory is a CP¹ gauge model, which is described by the following action S_z in the continuum space time with coordinate $x_\mu = (x_0 = \tau, x_1, x_2)$,

$$S_z = \int d^3x \left[\frac{1}{g^2} \sum_\mu |D_\mu z|^2 + \frac{1}{e^2} \sum_{\mu < \nu} F_{\mu\nu}^2 \right], \quad (2.6)$$

where $D_\mu z = (\partial_\mu + iA_\mu)z$ and $F_{\mu\nu} = \partial_\mu A_\nu - \partial_\nu A_\mu$ with emergent gauge field A_μ . In Eq. (2.6), g and e are coupling constants. Bare value of g is independent of the antiferromagnetic (AF) exchange coupling J but it measures the solidity of the AF order, i.e., additional interactions that enhance (suppress) the AF order decrease (increase) the value of g . On the other hand, the bare value of $1/e$ is vanishing for the AF Heisenberg model with only the nearest-neighbor (NN) coupling but it acquire a finite value due to the renormalization effect of the high-energy modes. Multispin nonlocal interactions such as a ring exchange coupling generate nonvanishing value of $1/e$.¹⁴ Varying the parameters g and e induces a phase transition and the structure of the ground-state and low-energy excitations change drastically through the phase transition as we see in the following sections.

The field theory defined by Eq. (2.6) is obviously invariant under a U(1) gauge transformation. The continuum description [Eq. (2.6)] makes it unclear if this U(1) gauge symmetry is compact or noncompact one. As the original system of the AF magnets is defined on the lattice and transformation parameter $\theta_i(\tau)$ is defined mod 2π , one may expect that the model (2.6) is a compact U(1) gauge system, in which topological nontrivial objects such as instantons and vortices

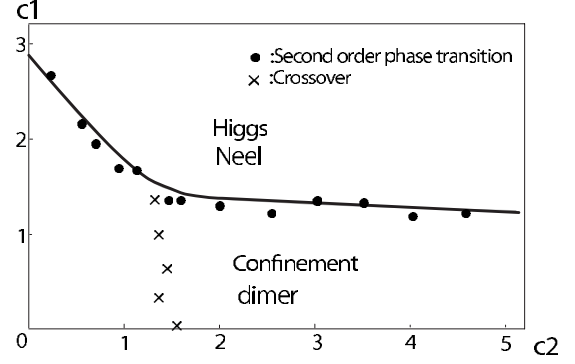


FIG. 2. Phase diagram of the U(1) gauge theory of CP¹ spinons (Ref. 20). There are two phases.

can exist. This expectation is qualitatively correct but contribution from instanton configurations to the partition function is partly suppressed if there exists a Berry-phase term, $\int d^3x \epsilon_{\mu\nu\lambda} \partial_\mu F_{\nu\lambda}$ (where $\epsilon_{\mu\nu\lambda}$ is the antisymmetric tensor, in the action in addition to S_z .^{15–17} For the case $J' \neq 0$, it is not easy to calculate the coefficient of the Berry phase, which plays a crucial role in the suppression of instantons. We shall not consider its effect in the following numerical investigation and give comments on it in Sec. IV.¹⁸

Phase structure of the CP^{N-1} field theory has been studied by the $1/N$ expansion and numerical methods.^{19–21} For the compact U(1) gauge case, a lattice-regularized version of Eq. (2.6) is quite useful for investigation on the CP¹ gauge model, and its action is given as follows:

$$A_z = \frac{c_1}{2} \sum_{x,\mu} \bar{z}_{x+\mu} U_{x,\mu} z_x + \frac{c_2}{2} \sum_{x,\mu < \nu} U_{x,\mu} U_{x+\mu,\nu} \bar{U}_{x+\nu,\mu} \bar{U}_{x,\nu} + \text{c.c.}, \quad (2.7)$$

where x denotes site of the *cubic lattice*, and the coupling c_1 corresponds to $1/g^2$ and c_2 to $1/e^2$. Phase diagram has been obtained in the c_1 - c_2 plane. See Fig. 2. There are two phases separated by the critical line $c_1 = c_{1c}(c_2)$, one of which corresponds to the Néel state for $c_1 > c_{1c}(c_2)$ and the other state is a dimer state $c_1 < c_{1c}(c_2)$ in which the spinon z_x is confined to a spin-triplet excitation $\bar{z}_x \vec{\sigma} z_x$. The phase transition across the transition line is of second order, and it belongs to the universality class of the O(3) nonlinear sigma model in three dimensions (3D) (for small to medium values of c_2). The $s = \frac{1}{2}$ AF Heisenberg model corresponds to $c_1 > c_{1c}$, and the ground state has the AF long-range order. By introducing an *inhomogeneity* in the exchange coupling J that enhances dimerization, the value of c_1 in the effective model (2.7) is decreased and the phase transition takes place from the Néel to dimer states.²² Recently, numerical study on the inhomogeneous SU(2) AF Heisenberg model, which is essentially the same with that studied in Ref. 22, was performed quite in detail and the existence of the phase transition from the Néel to dimer states was verified.²³ Phase transition belongs to the universality class of the 3D O(3) nonlinear sigma model, as predicted by the study of the effective lattice model (2.7).

As shown in Fig. 2, the deconfined Coulomb phase does not exist in the model (2.7) of the U(1) gauge theory. Ap-

pearance of the Coulomb phase requires long-range and non-local interaction of gauge field $U_{x\mu}$, which may be generated by the coupling with gapless fermions.^{24,25} In the pure quantum spin models without doping of holes, the deconfined phase is expected to appear by introducing frustrations because the Higgs mechanism is expected to take place by the appearance of the (short-range) spiral order. In that case, the U(1) gauge symmetry spontaneously breaks down to Z_2 . It is known that the deconfined phase exists in the 3D Z_2 gauge models. There are interesting studies on spin liquids with deconfined spinons in the framework of the Z_2 gauge model. However, detailed and reliable study on the phase structure of the Z_2 gauge models relevant to the frustrated spin systems is still lacking. We study this problem in this paper.

Before going into details of the study on the frustrated AF magnets, let us comment on the validity of the present methods using the lattice field theory for studying AF magnets. To define quantum many-body systems without ambiguities, an ultraviolet (UV) regularization is necessary. In quantum spin models such as (2.1), the spatial lattice naturally gives such an UV regularization. In the present approach, we first study the original model carefully and identify the relevant modes in the low-energy and low-momentum region. Through these observations, we obtain an effective-field theory in the continuum space time. Then in order to study the effective-field theory nonperturbatively (e.g., by means of the MC simulations), we reformulate it by using a *space-time* lattice as a systematic regularization. Structure of the lattice model is determined by the symmetry of the effective-field theory and we expect that details of the lattice model does not influence substantially physical results such as phase structure and critical behaviors by the universality-class argument. For the quantum SU(2) AF magnets, it is known that the results obtained by the effective CP¹ lattice model (2.7) are in good agreement with those obtained for the original AF Heisenberg model, as we explained above. Furthermore, phase structure of the lattice CP^{*n*} ($n=1, \dots, 4$) models obtained by the MC simulations is the same with that obtained by the $1/N$ expansion for the CP^{*N*-1} field theory in the continuum space time.^{19,20} These facts encourage us to apply the same methods to more complicated quantum spin systems such as triangular AF spin systems with frustrations. More comments on the reliability of the methods will be given in Sec. IV, after showing the main results of the present study in the following sections.

B. Effect of frustrations

The effect of the frustration in the AF magnets [Eq. (2.1)] can be studied in the framework of the CP¹ gauge-field theory whose action has the following term S_Λ in addition to S_z ,¹¹

$$S_\Lambda = \int d^3x \sum_{\alpha=1,2} \left[\frac{1}{g_\Lambda^2} |D_\mu^{(2)} \Lambda_\alpha|^2 + m_\Lambda |\Lambda_\alpha|^2 + \lambda |\Lambda_\alpha|^4 + i \Lambda_\alpha \bar{z} \partial_\alpha \bar{z} + \text{c.c.} \right], \quad (2.8)$$

where $\Lambda_\alpha (\alpha=1,2)$ is a *doubly charged spatial vector field*,

$D_\mu^{(2)} = \partial_\mu + 2iA_{\mu\alpha}$, and $\bar{z}_a(x) = \epsilon_{ab} \bar{z}_b(x)$ ($\epsilon_{12} = -\epsilon_{21} = 1$, $\epsilon_{11} = \epsilon_{22} = 0$). Origin of the new term S_Λ is as follows. The J' term in Eq. (2.1) generates terms such as $\frac{J'}{J} \sum_{ij} |\bar{z}_i \cdot \bar{z}_j|^2$ in the effective-field theory, where the extra factor $1/J$ comes from the redefinition of the imaginary time $\tau \rightarrow \tau \times (aJ)$ (a =lattice spacing=often set unity). After inserting the following identity into the path-integral representation of the partition function,

$$\int d\Lambda_{ij} d\bar{\Lambda}_{ij} e^{-J'/J \sum_{ij} \Lambda_{ij} \bar{z}_i \cdot \bar{z}_j} (J/J' \bar{\Lambda}_{ij} \bar{z}_i \cdot \bar{z}_j) = \text{constant} \quad (2.9)$$

the above quartic term of z_i is decoupled by a Hubbard-Stratonovich field Λ_α . By the effects of renormalization of high-momentum modes, the extra terms in S_Λ and renormalization of the mass, which preserve the local U(1) gauge symmetry, appear for describing low-energy behavior of the system.²⁶

Physical meaning of S_Λ becomes transparent by considering the case $m_\Lambda < 0$. In this case, we expect the nonvanishing expectation value of the field Λ_α , i.e., $\langle \Lambda_\alpha \rangle \neq 0$. By solving the field equation derived from the action $S_z + S_\Lambda$, it is straightforward to verify that the low-energy configurations are given by

$$z_a(x) = \frac{1}{\sqrt{2}} [v_a(x) e^{ig^2 \langle \bar{\Lambda} \rangle \cdot \vec{x}} + \epsilon_{ab} \bar{v}_b(x) e^{-ig^2 \langle \bar{\Lambda} \rangle \cdot \vec{x}}], \quad (2.10)$$

where $v_a(x)$ ($a=1,2$) is a slowly varying complex field satisfying $\sum_a |v_a(x)|^2 = 1$.^{27,28} For the configurations given by Eq. (2.10), the SU(2) spin field $\vec{S}(x) \equiv \bar{z}(x) \vec{\sigma} z(x)$ has the following form:

$$\vec{S}(x) = \vec{n}_1 \cos(2g^2 \langle \bar{\Lambda} \rangle \cdot \vec{x}) + \vec{n}_2 \sin(2g^2 \langle \bar{\Lambda} \rangle \cdot \vec{x}),$$

$$\vec{n}_1 = \text{Re}[\bar{v} \vec{\sigma} v], \quad \vec{n}_2 = \text{Im}[\bar{v} \vec{\sigma} v],$$

$$\vec{n}_1^2 = \vec{n}_2^2 = 1, \quad \vec{n}_1 \cdot \vec{n}_2 = 0. \quad (2.11)$$

On the other hand, the ‘‘spin-nematic field’’ $\vec{n}_3 = \vec{n}_1 \times \vec{n}_2$ is given as $\vec{n}_3 = \bar{v} \vec{\sigma} v$. It is obvious that $\vec{S}(x)$ in Eq. (2.11) corresponds to a spiral state if $\langle \vec{n}_1 \rangle \neq 0, \langle \vec{n}_2 \rangle \neq 0$.

By substituting Eq. (2.10) and $\Lambda_{0\alpha} = \langle \Lambda_\alpha \rangle$ into the continuum action $S_z + S_\Lambda$, low-energy effective theory is obtained. Condensation of Λ_α not only generates the spiral state of \vec{S} but also a finite mass of the gauge field A_μ . CP^{*N*-1} model with a massive ‘‘gauge field’’ has been studied in the continuum space time by the $1/N$ expansion but the obtained results are not reliable for the case of finite N (in particular, the case $N=2$) because an important effect at $O(1/N)$ coming from topological excitations is totally ignored there.²⁹ In fact, the condensation of Λ_α preserves the local Z_2 gauge invariance of the system because it carries double charge, and therefore the topological nontrivial excitation carrying a half-magnetic quantum, dubbed vison, exists as a low-energy excitation.³⁰ Also in Ref. 31, a quantum phase transition between a spin liquid with deconfined spinons and magnetically ordered state was studied, and various physical quantities were calculated by the $1/N$ expansion in an effec-

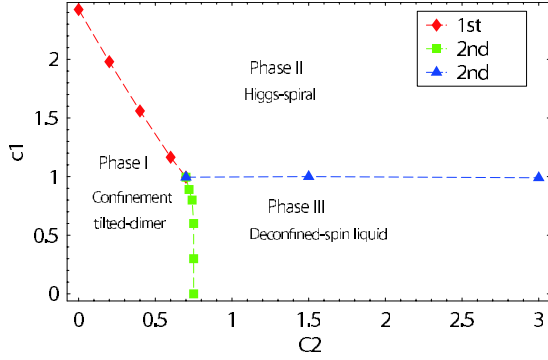


FIG. 3. (Color online) Phase diagram of the Z_2 gauge theory of CP^1 spinons. There are three phases.

tive CP^{N-1} field theory with a global $U(1)$ symmetry. There it is assumed that effect of the vision can be ignored. Our study of the gauge model with the full Z_2 gauge symmetry in the present paper will show that this assumption is correct. See, for example, the calculation of the instanton density in Sec. III.

In the rest of the present paper, we shall study the effective Z_2 gauge theories obtained by substituting $\vec{\Lambda} = \langle \vec{\Lambda} \rangle$ and Eq. (2.10) into the action $S_z + S_\Lambda$. To this end, we reformulate it by using the lattice regularization that preserves the local Z_2 gauge symmetry. We use a cubic space-time lattice because frustrations coming from AF coupling on the triangular lattice have disappeared by using the parameterization [Eq. (2.10)]. The resultant lattice model is explicitly given by the following action:

$$A(c_3) = \frac{c_1}{2} \sum_{x,\mu} (\bar{v}_{x+\mu} U_{x,\mu} v_x + \bar{v}_x U_{x,\mu} v_{x+\mu}) + \frac{c_2}{2} \sum_{x,\mu < \nu} U_{x,\mu} U_{x+\mu,\nu} \bar{U}_{x+\nu,\mu} \bar{U}_{x,\nu} + \frac{c_3}{2} \sum_{x,\mu} U_{x,\mu}^2 + c.c., \tag{2.12}$$

where we explicitly show the dependence of the parameter c_3 in $A(c_3)$, as we study the model with fixed values of c_3 in the following section. From the above consideration, $c_3 \propto \langle \vec{\Lambda} \rangle^2$. Partition function of the gauge model (2.12) is given as

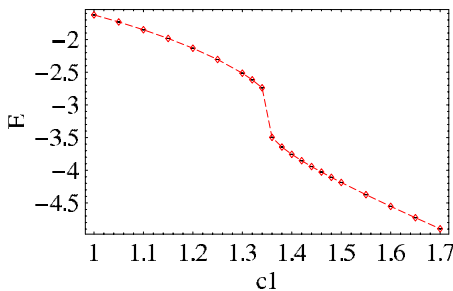
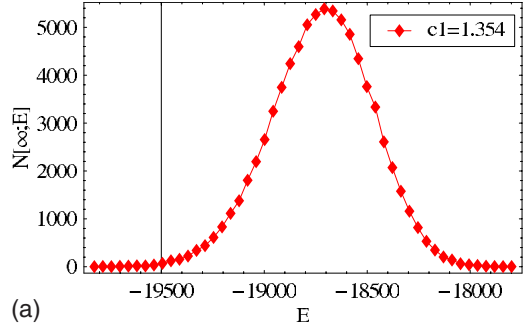
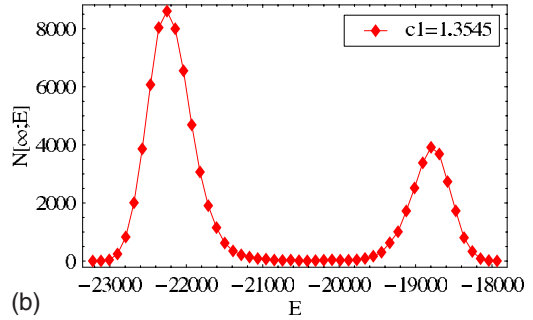


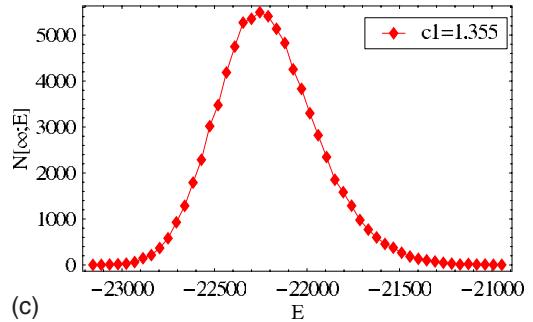
FIG. 4. (Color online) E for $c_2=0.5$. There is sharp discontinuity at $c_1 \approx 1.35$ that indicates a first-order phase transition. System size is $L=24$.



(a)



(b)



(c)

FIG. 5. (Color online) Distribution of $A(\infty)$ for $c_2=0.5$ and c_1 close to the phase transition point. The double-peak structure at $c_1=1.3545$ confirms the existence of the first-order phase transition. System size $L=24$.

$$Z_{\text{Gauge}} = \int [D\bar{z}Dz]_{CP^1} [D\bar{U}DU] \exp A(c_3). \tag{2.13}$$

It is obvious that the system (2.12) has a local Z_2 gauge symmetry instead of the $U(1)$ symmetry. Then we call v_x

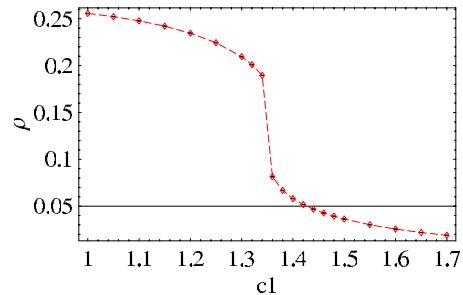


FIG. 6. (Color online) Instanton density for $c_2=0.5$ as a function of c_1 . At the phase transition point $c_1 \approx 1.35$, it changes its behavior. System size $L=24$.

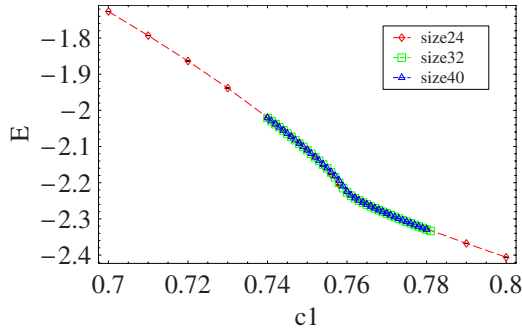


FIG. 7. (Color online) E for $c_1=0.3$ as a function of c_2 . System size $L=24,32,40$. There is almost no system-size dependence.

Z_2 CP¹ boson. In the limit $c_3 \rightarrow \infty$, configurations of the gauge field are restricted to $U_{x,\mu} = \pm 1$ and the model reduces to a Z_2 gauge system. In the case $c_3 \rightarrow \infty$, $c_1=0$, the system is the pure Z_2 gauge model in 3D, which is dual to the 3D Ising model and has a second-order phase transition from the confined to deconfined ‘‘Coulomb’’ phases as c_2 is increased. This is in sharp contrast to the U(1) gauge model in 3D, in which only the confined phase exists. As the deconfined phase corresponds to spin liquid with weakly interacting spinons, one may expect realization of a fractionalization phenomenon in frustrated AF magnets. In the following sections, we shall study phase structure of the model (2.12) by means of the MC simulations.

III. NUMERICAL STUDIES

A. Z_2 lattice gauge model of Z_2 CP¹ spinon

We first study the Z_2 gauge model coupled with the field v_x that corresponds to the limit $c_3 \rightarrow \infty$ of the model (2.12). It is known that Z_2 gauge model coupled with single-component Higgs boson describes nematic phase transition, and its phase structure was studied by both analytical and numerical methods.³² In these studies, importance of topological line defects (world lines of vortices) was emphasized.

In order to investigate the phase structure of the Z_2 gauge model, we defined the model on the cubic lattice of size L^3

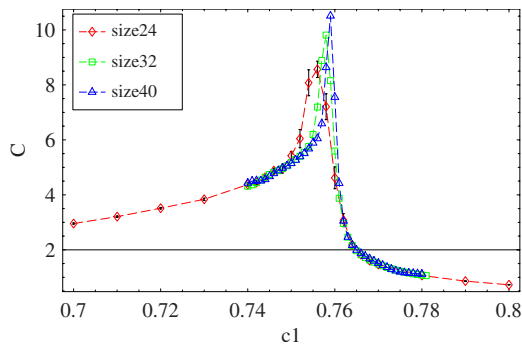


FIG. 8. (Color online) C for $c_1=0.3$ as a function of c_2 with $L=24,32,40$. Its system-size dependence indicates that the phase transition is of second order. In addition to the standard MC simulations, we used multihistogram methods to obtain reliable values of C near the phase transition point (Ref. 35).

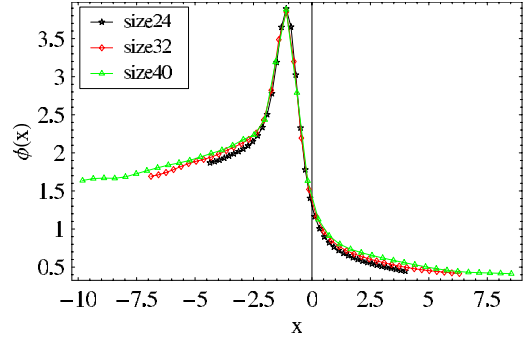


FIG. 9. (Color online) FSS for $c_1=0.3$. All data for $L=24,32,40$ can be fit by single function $\phi(x)$.

with the periodic boundary condition and calculated the internal energy $E = \langle A(\infty) \rangle / L^3$, the specific heat $C = \langle [A(\infty) - E]^2 \rangle / L^3$, etc. We used the standard Metropolis algorithm for the MC simulations.³³ The typical statistics used was 10^5 MC steps for each sample, and the averages and errors were estimated over 10–20 samples. Average acceptance probability was about 40–50 %.

The obtained phase diagram is shown in Fig. 3. There are three phases and calculation of various physical quantities gives the following identifications. (1) In the phase I, there is no AF long-range order and the gauge dynamics is realized in the confined phase. Low-energy excitations are spin-triplet bound states of the spinor v_x (triplon), i.e., $\vec{n}_1(x)$ and $\vec{n}_2(x)$ in Eq. (2.11). We call this phase tilted-dimer state. (2) In the phase II, there exists the magnetic long-range order of v_x , which corresponds to the spiral order of $\vec{S}(x)$, i.e., $\langle \vec{n}_1 \rangle \neq 0$ and $\langle \vec{n}_2 \rangle \neq 0$. The gauge dynamics is in the Higgs phase because of the condensation of v_x . Low-energy excitations are gapless spin wave described by *uncondensed component* of v_x . (3) Phase III represents the paramagnetic spin-liquid state. As for gauge dynamics, a deconfined ‘‘Coulomb phase’’ is realized and the number of topological vortices is conserved. Low-energy excitations are massive spinon v_x .

We first show the numerical calculations of E and C for establishing the above phase diagram in Fig. 3. We first focus on the transition from phase I to II. In Fig. 4, we show calculation of E as a function of c_1 with $c_2=0.5$. It is obvious that there exists a sharp discontinuity at $c_1 \approx 1.35$, which indicates a first-order phase transition. In order to verify it, we measured distribution of values of $A(\infty)$ generated in the MC steps, $\mathcal{N}[\infty; E]$, which is defined as

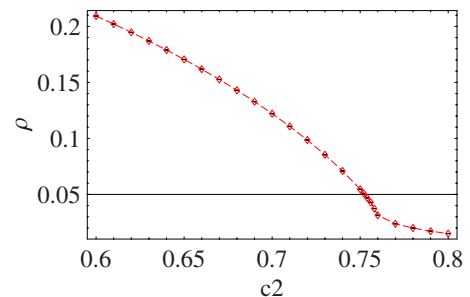


FIG. 10. (Color online) Instanton density for $c_1=0.3$ as a function of c_2 . At the phase transition point $c_2 \approx 0.76$, it changes its behavior. System size $L=24$.

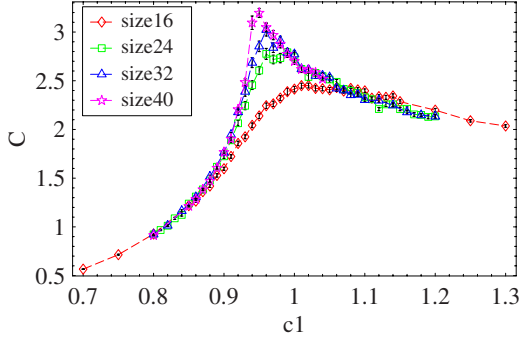


FIG. 11. (Color online) C for $c_2=1.5$ as a function of c_1 with $L=16,24,32,40$. Its system-size dependence indicates that the phase transition is of second order.

$$\begin{aligned} Z_{\text{Gauge}} &= \int dE \int [D\bar{Z}DZ]_{\text{CP}^1} [D\bar{U}DU] e^{A(\infty)} \delta[A(\infty) - E] \\ &= \int dE \mathcal{N}[\infty; E]. \end{aligned} \quad (3.1)$$

We show the result near the critical point in Fig. 5. At $c_1=1.3545$, $\mathcal{N}[\infty; E]$ has a double-peak structure whereas the others have a single peak. From this result, we judge that the first-order phase transition takes place at $c_1=1.3545$.

We also measured the instanton density $\rho(x)$ for $c_2=0.5$ as a function of c_1 . $\rho(x)$ is defined as follows for the gauge-field configuration $U_{x,\mu}=e^{i\theta_{x,\mu}}$, $\theta_{x,\mu}=0, \pi$.^{20,34} First we consider the magnetic flux $\Theta_{x,\mu\nu}$ penetrating plaquette $(x, x+\mu, x+\mu+\nu, x+\nu)$,

$$\Theta_{x,\mu\nu} = \theta_{x,\mu} + \theta_{x+\mu,\nu} - \theta_{x+\nu,\mu} - \theta_{x,\nu}, \quad (-2\pi \leq \Theta_{x,\mu\nu} \leq 2\pi). \quad (3.2)$$

We decompose $\Theta_{x,\mu\nu}$ into its integer part $n_{x,\mu\nu}$, which represents the Dirac string (vortex line) and the remaining part $\tilde{\Theta}_{x,\mu\nu}$

$$\Theta_{x,\mu\nu} = 2\pi n_{x,\mu\nu} + \tilde{\Theta}_{x,\mu\nu} \quad (-\pi \leq \tilde{\Theta}_{x,\mu\nu} \leq \pi). \quad (3.3)$$

Then instanton density $\rho(x)$ at the cube around the site $x + \frac{0}{2} + \frac{1}{2} + \frac{2}{2}$ of the dual lattice is defined as

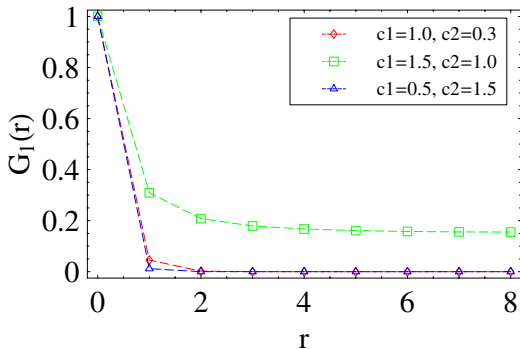


FIG. 12. (Color online) Correlation function of the spin field $\tilde{n}_1(x)$. It has a long-range order only in phase II.

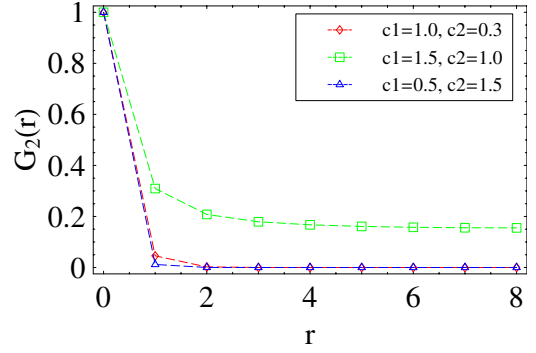


FIG. 13. (Color online) Correlation function of the spin field $\tilde{n}_2(x)$. It has a long-range order only in phase II.

$$\begin{aligned} \rho(x) &= -\frac{1}{2} \sum_{\mu\nu\lambda} \epsilon_{\mu\nu\lambda} (n_{x+\mu,\nu\lambda} - n_{x,\nu\lambda}) \\ &= \frac{1}{4\pi} \sum_{\mu\nu\lambda} \epsilon_{\mu\nu\lambda} (\tilde{\Theta}_{x+\mu,\nu\lambda} - \tilde{\Theta}_{x,\nu\lambda}), \end{aligned} \quad (3.4)$$

where $\epsilon_{\mu\nu\lambda}$ is the antisymmetric tensor. From the above definition, it is obvious that $\rho \equiv \langle |\rho(x)| \rangle$ measures probability of creation/annihilation of magnetic vortex. In 3D Z_2 gauge theory, magnetic vortices in 3D can be regarded as world lines of flux quanta dubbed vision. Nonvanishing value of ρ means that the number of visions is not conserved and therefore *condensation of the vision*. The result of calculation of ρ is shown in Fig. 6. There is a sharp discontinuity at the phase transition $c_1 \approx 1.35$. In phase I, finite value of ρ means large fluctuations of the gauge field and spinon v_x is confined to gauge-invariant composites, $\tilde{n}_i (i=1,2,3)$. This phenomenon is sometimes called *dual Meissner effect*. On the other hand in phase II, ρ is strongly suppressed and the topological order exists. Later study on the spin-correlation function reveals that this suppression is due to Higgs mechanism by the condensation of v_x .

Next we consider the phase transition from phase I to III. We show E and C for $c_1=0.3$ in Figs. 7 and 8. The results indicate that there exists a second-order phase transition at $c_2 \approx 0.76$. By the finite-size scaling (FSS) hypothesis for C ,

$$C_L(\epsilon) = L^{\sigma/\nu} \phi(L^{1/\nu} \epsilon), \quad (3.5)$$

where C_L is the specific heat of system size L , and $\epsilon \equiv (c_2 - c_{2\infty})/c_{2\infty}$ with $c_{2\infty}$ (the critical coupling for $L \rightarrow \infty$), we es-

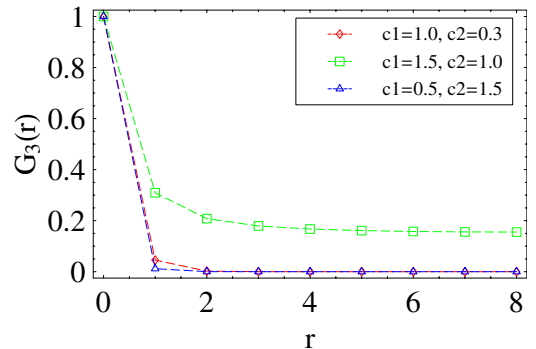
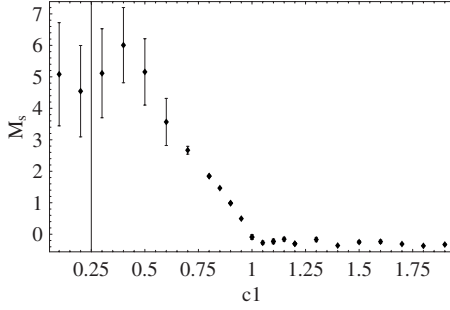


FIG. 14. (Color online) Correlation function of the spin-nematic field $\tilde{n}_3(x)$. It has a long-range order only in phase II.


 FIG. 15. Spin gap as a function of c_1 for $c_2=1.5$.

timated the critical exponents ν and σ by using the FSS [Eq. (3.5)] and obtained $\nu=0.63$ and $\sigma=0.17$ and the critical coupling $c_{2\infty}=0.76$. The obtained scaling function $\phi(x)$ is shown in Fig. 9. These values are very close to those of the pure Z_2 gauge model that are obtained from the data of the 3D Ising model by duality.³⁶

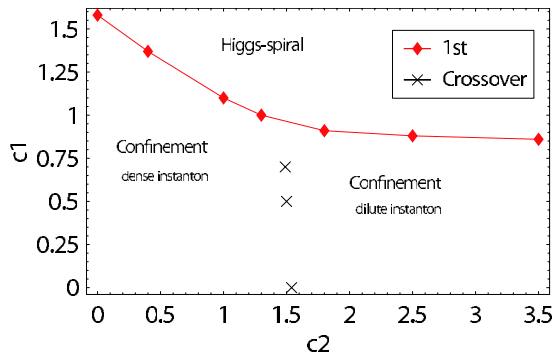
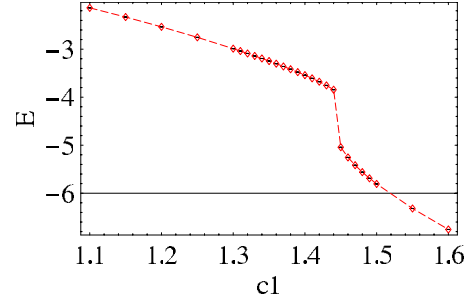
We also measured instanton density ρ and show the result in Fig. 10. ρ is a decreasing function of c_2 and changes its behavior at the phase transition point $c_2 \approx 0.76$.

Finally, let us consider the phase transition from the phases II to III. Obtained E has no system-size dependence. System-size dependence of C is shown in Fig. 11, from which we judge that the phase transition is of second order. By the FSS, the critical exponents are estimated as $\nu=0.65$, $\sigma=0.156$, and $c_{2\infty}=0.93$. This value of ν should be compared with that of the $O(4)$ nonlinear sigma model in 3D, $\nu_{O(4)}=0.75$. At present, it is not clear for us if the above two phase transitions belong to the same universality class.

In order to see (non)existence of the magnetic LRO, we measured correlation functions of the spins $\tilde{n}_1(x)$, $\tilde{n}_2(x)$, and $\tilde{n}_3(x)$. They are defined as

$$G_i(r) = \frac{1}{L^3} \sum_x \langle \tilde{n}_i(x+r) \cdot \tilde{n}_i(x) \rangle, \quad i = 1, 2, 3. \quad (3.6)$$

We exhibit the results in Figs. 12–14. It is obvious that only in phase II, they have the LRO. This LRO indicates a non-vanishing expectation value of v_x , $\langle v_x \rangle \neq 0$, in phase II. This understanding is supported by the measure of ρ , which shows that the gauge dynamics is in the Higgs phase in phase II.


 FIG. 16. (Color online) Phase diagram of the U(1) gauge theory of CP^1 spinons with $c_3=0$. There are two phases.

 FIG. 17. (Color online) E for $c_2=0.4$. There is sharp discontinuity at $c_1=1.44$ that indicates a first-order phase transition. System size is $L=24$.

We also calculated the spin gap as a function c_1 for $c_2 = 1.5$, i.e., from the spin liquid to spiral state. It is difficult to estimate the spin gap directly from the spin-correlation functions $G_i(r)$. Then as in the previous studies,²⁰ we employ a Fourier transformation of the spin field, e.g., $\tilde{n}_3(x)$,

$$\tilde{n}_3(x_0; p_1, p_2) = \sum_{x_1, x_2} e^{ip_1 x_1 + ip_2 x_2} \tilde{n}_3(x). \quad (3.7)$$

In the continuum limit, the correlator of $\tilde{n}_3(x_0; p_1, p_2)$ behaves as

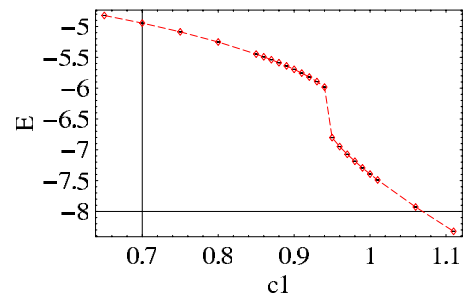
$$\langle \tilde{n}_3(x_0; p_1, p_2) \cdot \tilde{n}_3(0; p_1, p_2) \rangle = \int dp_0 \frac{e^{ip_0 x_0}}{\tilde{p}^2 + M_s^2} \propto e^{-\sqrt{p_1^2 + p_2^2 + M_s^2} x_0}, \quad (3.8)$$

where $\tilde{p}^2 = \sum_{i=1,2,3} p_i^2$. In the practical calculation on the lattice, we put $p_1 = p_2 = 2\pi/L$, and measured $\sqrt{p_1^2 + p_2^2 + M_s^2}$ from the correlation function of $\tilde{n}_3(x_0; p_1, p_2)$. We show the result M_s as a function of c_1 in Fig. 15. It is obvious that the spin gap M_s is a continuous decreasing function of c_1 and is vanishing for $c_1 > c_{1c} \approx 1$. This result means that the spin excitation has a finite gap in the Z_2 spin liquid whereas the spin wave in the spiral state is gapless.

From all the above calculations, we obtain the phase diagram shown in Fig. 3.

B. U(1) gauge field coupled to $Z_2 CP^1$ spinon: $c_3=0$ case

Let us consider the case $c_3=0$ of the system (2.12). The system with $c_1=0$ is nothing but the pure compact U(1)


 FIG. 18. (Color online) E for $c_2=1.8$. There is sharp discontinuity at $c_1=0.95$ that indicates a first-order phase transition. System size is $L=24$.

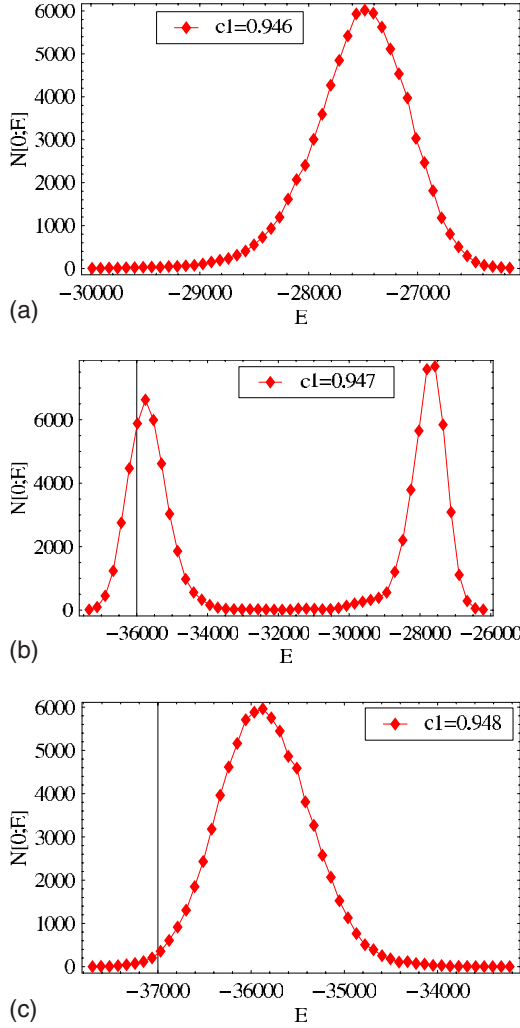


FIG. 19. (Color online) Distribution of $A(0)$ for $c_2=1.8$ and c_1 close to the phase transition point. The double-peak structure at $c_1=0.947$ confirms the existence of the first-order phase transition. System size $L=24$.

gauge model in 3D. It is well known that there is no phase transition and the system is always in the confined phase, though there is a crossover from dense-instanton to dilute-instanton regimes as the parameter c_2 is increased.

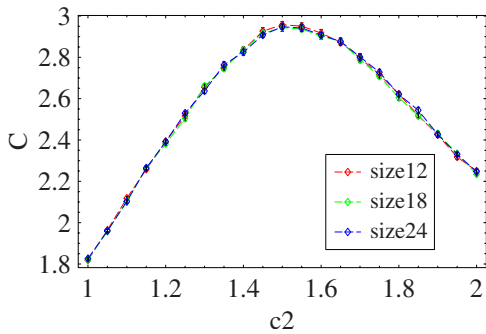


FIG. 20. (Color online) C for $c_1=0.5$. System size $L=12, 18, 24$. There is no system-size dependence, i.e., the second-order phase transition in the Z_2 gauge model reduces to a crossover. The deconfined spin-liquid phase does not exist in the model with $c_3=0$.

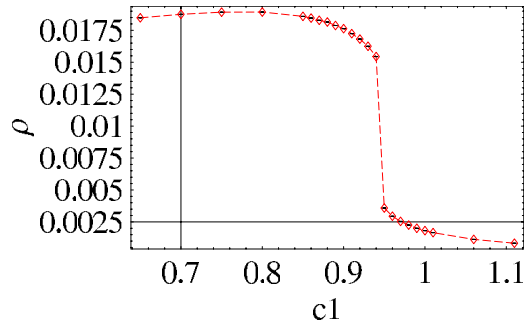


FIG. 21. (Color online) Instanton density for $c_2=1.8$ as a function of c_1 . At the phase transition point $c_1 \approx 0.95$, there is a sharp discontinuity. System size $L=24$.

We show the obtained phase diagram of the system (2.12) with $c_3=0$ in Fig. 16. There are two phases, (i) phase I is the dimer phase with confinement of spinons and without any long-range order and (ii) phase II is the spiral state with the condensation of v_x . Phase transitions separating these two phases are of first order as the calculations of E in Figs. 17 and 18 indicates. In order to verify this observation, we measured the distribution of $A(0)$, $\mathcal{N}[0;E]$, in the MC steps. From Fig. 19, it is obvious that on the critical line $\mathcal{N}[0;E]$ has a double-peak structure whereas it does not off the critical line.

The second-order phase transition that exists in the Z_2 gauge model of spinons from the confined to deconfined phases disappears in the system with $c_3=0$. There is a crossover line emanating from the crossover point of the pure compact $U(1)$ gauge model in 3D. See Fig. 20. This fact strongly influences structure of the ground-state and low-energy excitations of the original spin system. Absence of the deconfined phase means that *the spin-liquid phase does not exist* in the present case. We measured the instanton density ρ to verify the above conclusion. In particular, in the dilute-instanton regime $c_2 > 1.5$, the instanton density ρ is small even in the confined phase $c_1 < c_{1c}(c_2)$ but it decreases rapidly at the phase transition $c_1 = c_{1c}(c_2)$ to the Higgs phase. See Fig. 21. On the other hand for $c_1=0.5$, ρ is a decreasing function of c_2 but does not exhibit any anomalous behavior at the crossover $c_2 \approx 1.5$. See Fig. 22.

We calculated the spin-correlation functions in each phase and verified that the spin LRO exists only in the Higgs phase $c_1 > c_{1c}$.

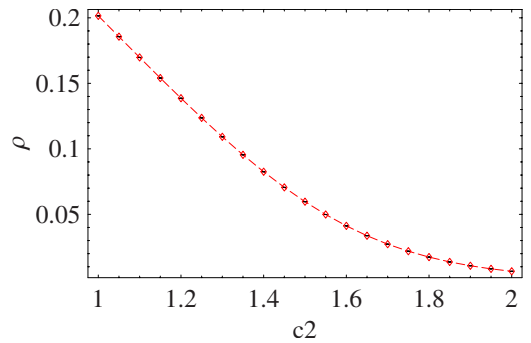


FIG. 22. (Color online) Instanton density for $c_1=0.5$ as a function of c_2 . There is no anomalous behavior at the crossover $c_2 \approx 1.5$. System size $L=24$.

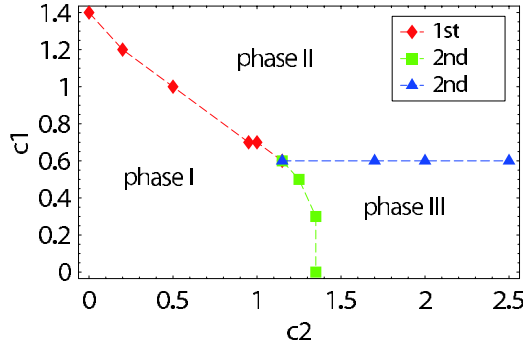


FIG. 23. (Color online) Phase diagram of the U(1) gauge theory of CP^1 spinons with $c_3=1.0$. There are three phases as in the Z_2 gauge model.

C. Massive U(1) gauge field coupled with Z_2CP^1 spinon: $c_3=1.0$ case

Finally let us consider the case $c_3=1.0$. We also investigated the case $c_3=2.0$ and obtained similar results. In the present case $c_3>0$, the gauge field $U_{x,\mu}$ is a $U(1)$ variable but local $U(1)$ gauge symmetry is explicitly broken down to Z_2 by both the hopping term of v_x and the mass term of the gauge field, i.e., $U_{x,\mu}^2+c.c.$ It is expected that the mass term of the gauge field is a relevant perturbation and therefore the phase structure of the system $c_3>0$ is qualitatively the same with that of the Z_2 gauge theory studied in Sec. III A.

We show the obtained phase diagram in Fig. 23. There are three phases similarly to the Z_2 gauge theory of spinons, as it is expected. In Figs. 24 and 25, we show C as a function of c_2 for $c_1=0.3$ and the FSS scaling function obtained from these data. Critical exponents are estimated as $\nu=1.26$, $\sigma=0.43$, and $c_{2\infty}=1.44$. From the above result, we think that the present phase transition does not belong to the universality class of the 3D Ising model. At phase transitions from the tilted-dimer to spiral phases, E , the distribution of $\mathcal{N}[1;E]$ and the instanton density ρ have similar behaviors to those in the previous cases of the first-order phase transition. In Figs. 26 and 27, we show the result of the instanton density.

IV. CONCLUSION AND DISCUSSION

In the present paper, we derived effective gauge models that describe low-energy properties of antiferromagnets with

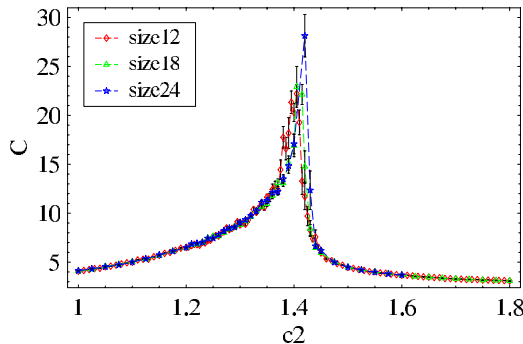


FIG. 24. (Color online) C for $c_1=0.3$. System size $L=12, 18, 24$.

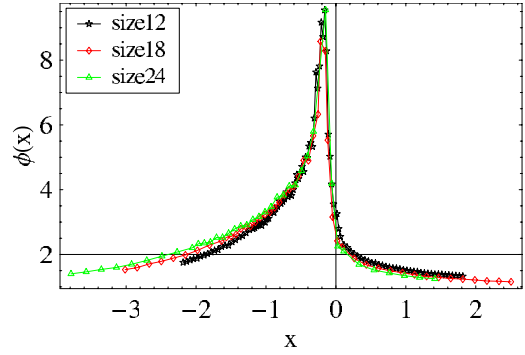


FIG. 25. (Color online) FSS for $c_1=0.3$. All data for $L=12, 18, 24$ can be fit by single function $\phi(x)$.

frustrations in two dimensions, and studied their phase structure mostly by means of MC simulations. We found that generally there are three phases in the models, (i) phase of the tilted-dimer state with spin-triplet excitations, (ii) the spiral state with gapless spin wave, and (iii) the spin liquid with weakly interacting spinons. We identified the order of the phase transitions and estimated values of the critical exponents of the second-order phase transitions. The investigation suggests that for the spin liquid to appear, multispin and nonlocal interactions are necessary in the original spin systems.

In order to verify the validity of the above results, it is important and also possible to study spin systems on layered 3D triangular lattice at finite temperature (T) by means of the Schwinger-boson (CP^1) representations. In this case, the systems can be studied directly with the spatial lattice as a regularization. In the path-integral representation of the partition function Z in Eq. (2.5) at finite T , the τ dependence of z_i is ignored. Then the path integral over CP^1 variables z_i 's in Z can be performed without any difficulties by the MC simulations. At present we are studying these systems, and have obtained preliminary results that support the conclusion in the present paper.³⁷

In the present paper, we mostly focus on the (short-range) spiral state with $\langle \Lambda_{ij} \rangle \propto \langle z_i \cdot \bar{z}_j \rangle = \Lambda_0 \neq 0$. There is another possibility of canted state such as $\langle \Lambda_{i,i+\hat{i}} \rangle = (-)^i \Lambda_0 \neq 0$. This state can be regarded as a state with a ferromagnetic order in the AF background. This state also breaks the $U(1)$ gauge invari-

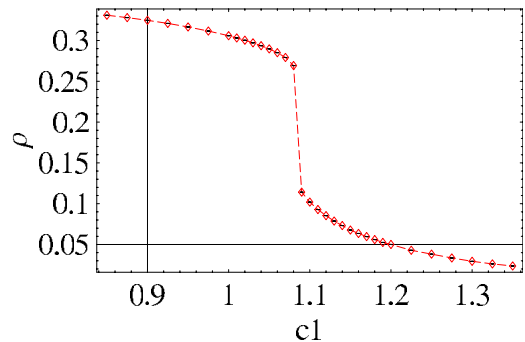


FIG. 26. (Color online) Instanton density for $c_2=0.5$ as a function of c_1 . At $c_1 \approx 1.1$, there is sharp discontinuity corresponding to the first-order phase transition. System size $L=24$.

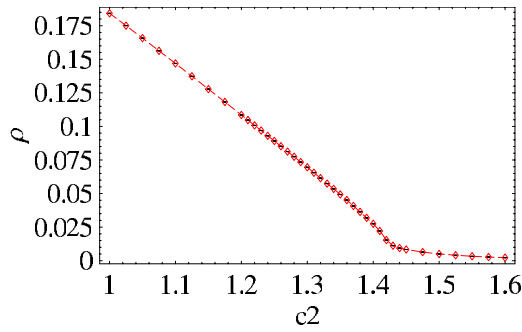


FIG. 27. (Color online) Instanton density for $c_1=0.3$ as a function of c_2 . At $c_2 \approx 1.4$, ρ changes its behavior. System size $L=24$.

ance down to the Z_2 as the (short-range) spiral state does, and therefore results obtained in the present paper are expected to be applicable to the canted state.

Finally let us comment on effects of the Berry phase. As we explained in Sec. II, the Berry phase appears after integrating out the high-energy modes in the path integral in order to derive the effective-field theory of AF magnets. The Berry phase may play an important role though qualitative phase structure is not changed by its existence.³⁸ Whether the suppression of the instantons occurs by the Berry phase

strongly depends on its coefficient. For example, in the *inhomogeneous* AF Heisenberg model on a square lattice, the coefficient depends on the magnitude of the inhomogeneity and is generally an irrational.²² Suppression of instantons does not occur in that case and the Néel-dimer phase transition belongs to the universality class of the classical 3D O(3) nonlinear sigma model, which is equivalent to the CP¹ gauge model (2.6) *without* the Berry phase. This result was verified by the numerical study of the inhomogeneous SU(2) AF Heisenberg model. We expect that nonvanishing frustration coupling J' gives a similar effect on the Berry-phase's coefficient because the most dominant NN spin-pair configuration is shifted from $z_{ia} = \epsilon_{ab} \bar{z}_{jb}$ (i, j =site, a, b =spinor indices) on path-integrating out high-energy modes. If this is the case, the Berry phase gives only negligible effects on critical behavior of the systems under study, and the FSS used in the present paper gives reliable estimation of the critical exponents.⁴¹

ACKNOWLEDGMENT

This work was partially supported by Grant-in-Aid for Scientific Research from Japan Society for the Promotion of Science under Grant No.20540264.

- ¹See, for example, P. A. Lee, N. Nagaosa, and X.-G. Wen, *Rev. Mod. Phys.* **78**, 17 (2006).
- ²K. Miyagawa, A. Kawamoto, Y. Nakazawa, and K. Kanoda, *Phys. Rev. Lett.* **75**, 1174 (1995).
- ³T. Nakamura, T. Takahashi, S. Aonuma, and R. Kato, *J. Mater. Chem.* **11**, 2159 (2001).
- ⁴M. Tamura and R. Kato, *J. Phys.: Condens. Matter* **14**, L729 (2002).
- ⁵Y. Shimizu, H. Akimoto, H. Tsujii, A. Tajima, and R. Kato, *Phys. Rev. Lett.* **99**, 256403 (2007).
- ⁶Y. Shimizu, K. Miyagawa, K. Kanoda, M. Maesato, and G. Saito, *Phys. Rev. Lett.* **91**, 107001 (2003).
- ⁷S. Yamashita, Y. Nakazawa, M. Oguni, Y. Oshima, H. Nojiri, Y. Shimizu, K. Miyagawa, and K. Kanoda, *Nat. Phys.* **4**, 459 (2008).
- ⁸Y. Qi, C. Xu, and S. Sachdev, *Phys. Rev. Lett.* **102**, 176401 (2009).
- ⁹R. Coldea, D. A. Tennant, A. M. Tsvetlik, and Z. Tylczynski, *Phys. Rev. Lett.* **86**, 1335 (2001).
- ¹⁰R. Coldea, D. A. Tennant, and Z. Tylczynski, *Phys. Rev. B* **68**, 134424 (2003).
- ¹¹See, for example, S. Sachdev, *Nat. Phys.* **4**, 173 (2008), and references cited therein.
- ¹²D. P. Arovas and A. Auerbach, *Phys. Rev. B* **38**, 316 (1988).
- ¹³I. Ichinose and T. Matsui, *Phys. Rev. B* **45**, 9976 (1992).
- ¹⁴K. Sawamura, T. Hiramatsu, K. Ozaki, I. Ichinose, and T. Matsui, *Phys. Rev. B* **77**, 224404 (2008).
- ¹⁵F. D. M. Haldane, *Phys. Rev. Lett.* **61**, 1029 (1988).
- ¹⁶N. Read and S. Sachdev, *Nucl. Phys. B* **316**, 609 (1989).
- ¹⁷N. Read and S. Sachdev, *Phys. Rev. B* **42**, 4568 (1990).

- ¹⁸The effects of the Berry phase were studied by doubled Chern-Simons theories rather in details by C. Xu and S. Sachdev, *Phys. Rev. B* **79**, 064405 (2009).
- ¹⁹I. Ya. Aref'eva and S. I. Azakov, *Nucl. Phys. B* **162**, 298 (1980).
- ²⁰S. Takashima, I. Ichinose, and T. Matsui, *Phys. Rev. B* **72**, 075112 (2005).
- ²¹For numerical study on the noncompact CP¹ U(1) gauge model, see O. I. Motrunich and A. Vishwanath, *Phys. Rev. B* **70**, 075104 (2004).
- ²²D. Yoshioka, G. Arakawa, I. Ichinose, and T. Matsui, *Phys. Rev. B* **70**, 174407 (2004).
- ²³S. Wenzel and W. Janke, *Phys. Rev. B* **79**, 014410 (2009).
- ²⁴G. Arakawa, I. Ichinose, T. Matsui, and K. Sakakibara, *Phys. Rev. Lett.* **94**, 211601 (2005).
- ²⁵G. Arakawa, I. Ichinose, T. Matsui, K. Sakakibara, and S. Takashima, *Nucl. Phys. B: Field Theory Stat. Syst.* **B732[FS]**, 401 (2006).
- ²⁶Corresponding to the spin model (2.1), the only single-component $\Lambda_{\alpha=1}$ appears in the effective-field theory. However, here we also introduce $\Lambda_{\alpha=2}$ for general consideration.
- ²⁷More precisely, in order to introduce the new complex field $v(x)$ through Eq. (2.10), we have to fix the gauge. The most convenient one is, e.g., $\Lambda_1 = \text{real}$ for the case $\langle \Lambda_\alpha \rangle = \langle \Lambda_1 \rangle \delta_{\alpha 1}$.
- ²⁸From Eq. (2.10), it is obvious that a global U(1) phase rotation of $v(x)$ corresponds to a spatial translation.
- ²⁹P. Azaria, P. Lecheminant, and D. Mouhanna, *Nucl. Phys. B* **455**, 648 (1995).
- ³⁰T. Senthil and M. P. A. Fisher, *Phys. Rev. B* **63**, 134521 (2001).
- ³¹A. V. Chubukov, S. Sachdev, and T. Senthil, *Nucl. Phys. B* **426**, 601 (1994).

- ³²P. E. Lammert, D. S. Rokhsar, and J. Toner, Phys. Rev. Lett. **70**, 1650 (1993).
- ³³N. Metropolis, A. W. Rosenbluth, M. N. Rosenbluth, A. M. Teller, and E. Teller, J. Chem. Phys. **21**, 1087 (1953).
- ³⁴T. A. DeGrand and D. Toussaint, Phys. Rev. D **22**, 2478 (1980).
- ³⁵A. M. Ferrenberg and R. H. Swendsen, Phys. Rev. Lett. **63**, 1195 (1989).
- ³⁶See, for example, C. Itzykson and J.-M. Drouffe, *Statistical Field Theory* (Cambridge University Press, Cambridge, England, 1989), Chap. 6.
- ³⁷K. Nakane, T. Kamijo, I. Ichinose, and T. Matsui (unpublished).
- ³⁸The Berry phase may move the location of the phase transition point and also change the order of the phase transition from second to first (Refs. [39](#) and [40](#)).
- ³⁹A. B. Kuklov, N. V. Prokofev, B. V. Svistunov, and M. Troyer, Ann. Phys. **321**, 1602 (2006).
- ⁴⁰S. Kragset, E. Smørgrav, J. Hove, F. S. Nogueira, and A. Sudbø, Phys. Rev. Lett. **97**, 247201 (2006).
- ⁴¹One may think that by the condensation of \vec{A} , U(1) gauge field reduces to Z_2 and then the Berry phase becomes ineffective to instanton because discussion of instanton suppression in Refs. [16](#) and [17](#) is not directly applicable to the Z_2 gauge theory. However the instanton density can be defined without any ambiguity in the Z_2 gauge theory if we use the space-time lattice regularization. It is an interesting problem to see if the instanton suppression argument in the U(1) gauge theory survives in the Z_2 theory or not.